M. E. Brown
Rhodes University
Grahamstown 6140, South Africa

Determination of Purity by Differential Scanning Calorimetry (DSC)

Measurement of the depression of the freezing point of a sample is often used to determine its purity. Some of the problems associated with the definition of the purity of a substance have been discussed by Smit (*1*). He stresses that it is inadequate to specify only the fraction (usually mole percent) of the main component present, for identification of the impurities and investigation of their mode of incorporation in the solid and the nature of the melt formed are essential. Freezing-point depression calculations are usually based on the assumption that solid solutions are not formed and that the melt is an ideal solution. The practical aim of purity determinations is usually to decide whether the sample meets certain specifications which are determined by the intended further uses of the sample. Purity determination by cryoscopy was put on a more quantitative basis in the method of measuring the enthalpy of premelting (*2*) of a substance as a function of temperature, introduced by Johnston and Giauque (*3*). Large sample masses were used and long periods were required for establishment of thermal equilibrium. Both factors have been dramatically reduced (*4*) by the development of differential scanning calorimetry (DSC).

In differential scanning calorimetry (*5*) the energy required to maintain both a sample and an inert reference material at the same temperature throughout a programmed temperature change is recorded. During melting, energy has to be supplied to the sample. A melting endotherm for a pure substance is illustrated in Figure 1. T_0 is the freezing point of the sample, and the area *ABC* is proportional to the enthalpy of melting, ΔH_{melt} of the sample. The presence of an impurity in the sample (the solvent) generally lowers the freezing point of the solvent and also broadens the melting range, giving a broader DSC endotherm as illustrated in the inset in Figure 2. From endotherms such as illustrated in Figures 1 and 2, freezing points and enthalpies of melting may be determined readily. With more effort an estimate of the purity of a compound can be obtained, from analysis of *the detailed shape* of its melting endotherm, for example, Figure 2, without reference to compounds containing known amounts of impurities. The method is only satisfactorily applied for impurity levels below about 3 mole per cent.

Such an exercise has several educational advantages. It concentrates attention on some aspects of the thermodynamics of melting which are not often covered in detail in lecture courses. The experimental result, that is, lowering of the freezing point by impurities, is well known from introductory laboratory sessions, but is seen here in a new light with theory providing an "absolute" route to determination of sample purity. Attention is also focused on one of the important techniques of thermal analysis, DSC, and its versatility for estimating thermodynamic properties.

Since differential scanning calorimeters may not be widely accessible, data and references are provided to enable the exercise to be carried out as a "dry-lab" experiment.

The Melting Process

The simplest system to consider is that in which the impurity does not go into solid solution with the solvent, but forms an ideal solution in the melt, that is, a eutectic system. If the impurity is labelled, in the customary way, as component 2 and the solvent as component 1, then freezing-point depression calculations are based (*6*) on the expression for the mole fraction of solute (impurity) in the equilibrium melt at temperature, T

$$x_2 = \frac{\overline{\Delta H}^{\theta}_{\mathrm{melt},1}}{R}\left[\frac{1}{T} - \frac{1}{T_{\mathrm{o}}}\right] \tag{1}$$

where $\overline{\Delta H}^{\theta}_{\mathrm{melt},1}$ is the standard molar enthalpy of melting of the pure solvent, assumed to be independent of temperature over the range, and T_0 is the freezing point of the pure solvent.

At the unique temperature $T = T_{\mathrm{f}}$, the freezing point of the impure sample, the mole fraction of impurity is given by

$$x_2 = \frac{\overline{\Delta H}^{\theta}_{\mathrm{melt},1}}{R}\left[\frac{T_{\mathrm{o}} - T_{\mathrm{f}}}{T_{\mathrm{o}}T_{\mathrm{f}}}\right] = \frac{\overline{\Delta H}^{\theta}_{\mathrm{melt},1}}{R}\cdot\frac{\Delta T_{\mathrm{f}}}{T_{\mathrm{o}}T_{\mathrm{f}}} \tag{2}$$

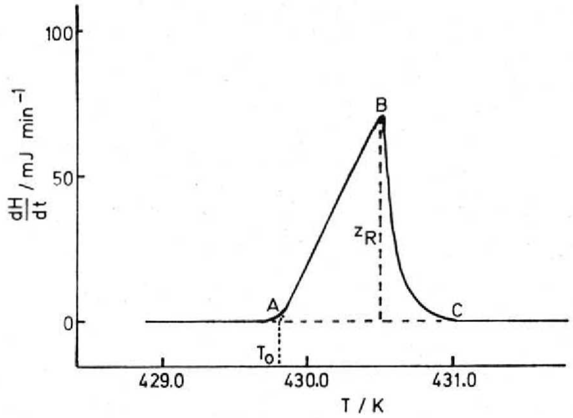

Figure 1. Idealized DSC record of melting of 0.01 mmol of very pure indium metal (heating rate, $\phi = 1$ K min^{-1}). The slope of *AB* (= $1/R_{\mathrm{o}}$) is used to correct for thermal lag. T_{o} is the melting point. Area *ABC* represents the enthalpy of melting, $\overline{\Delta H}^{\theta}_{\mathrm{melt,In}}$. z_R is the maximum value of the apparent heat capacity of this reference material (see text).

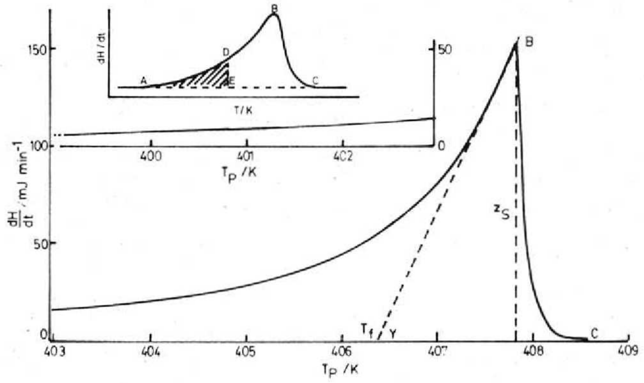

Figure 2. Idealized DSC record of melting of 0.01 mmol of an impure sample of phenacetin (heating rate, $\phi = 1$ K min^{-1}). The slope of *YB* (= slope of *AB* in Fig. 1) is used to correct the programmed temperature, T_{P}, to the sample temperature, T_{S}. ($T_{\mathrm{S}} = T_{\mathrm{P}} - YW$). T_{f} is the freezing point. The area ABC represents the enthalpy of melting of phenacetin, $\overline{\Delta H}^{\theta}_{\mathrm{melt},1}$. The fraction melted, F_{n}, at temperature, T_{n}, is equal to (area ADE/(area ABC)). z_S is the maximum value of the apparent heat capacity of the sample (see text).

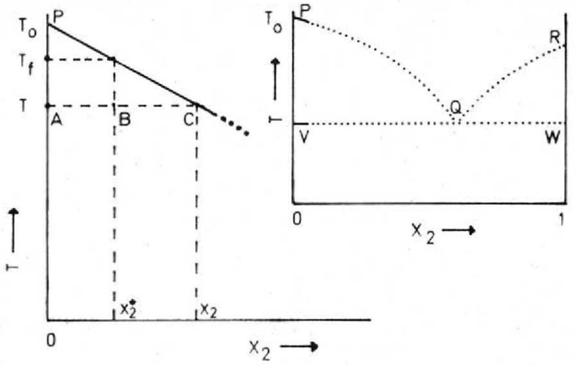

Figure 3. Low concentration region ($x_2 < 0.05$) of a simple eutectic phase diagram (inset). By the lever rule: $BC/AB = n_{solid}/n_{liquid}$. C is the composition of the melt in equilibrium with pure solid at T. Here $x_2 > x_2^*$. The fraction of sample melted $F = n_l/(n_s + n_l) = AB/(AB + BC) = AB/AC = x_2^*/x_2$.

If the depression of the freezing point, ΔT_f, is small, $T_o \simeq T_f$ so that $T_oT_f \simeq T_o^2$. Also $x_2 = n_2/(n_1 + n_2) \simeq mM_1/1000$, where m is the molarity of solute and M_1 the molar mass of the solvent. Hence

$$\Delta T_f = \left[\frac{RT_o^2 M_1}{\overline{\Delta H}^{\theta}_{\mathrm{melt},1}\,(1000)}\right] m = K_f \cdot m$$

where K_f is termed the cryoscopic constant.

The above relationships apply only to low impurity levels ($x_2 < 0.03$), that is, to the extremity of the liquidus curve, PQ, of the simple eutectic phase diagram (Figure 3, inset), shown on a much enlarged scale in Figure 3.

Only when the sample is completely melted, at $T > T_f$, is the mole fraction of impurity in the liquid, x_2, the same as that in the original sample, x_2^*. The value x_2^* is the minimum value which x_2 attains. At $T < T_f$, when the fraction of sample that has melted, F, is less than unity, $x_2 > x_2^*$. Assuming a linear initial segment of the liquidus curve, PQ, and using eqn. (1)

$$F = \frac{x_2^*}{x_2} = \frac{T_o - T_f}{T_o - T} = \frac{x_2^* R T_o}{\overline{\Delta H}^{\theta}_{\mathrm{melt},1}\,(T_o - T)} \tag{3}$$

Rearrangement yields

$$T = T_o - \left[\frac{x_2^* R T_o^2}{\overline{\Delta H}^{\theta}_{\mathrm{melt},1}}\right]\frac{1}{F} \tag{4}$$

If F can be determined at various temperatures, T, a plot of T against $1/F$ should yield a straight line, provided that $\overline{\Delta H}^{\theta}_{\mathrm{melt},1}$ is independent of temperature. If the values of T_o and $\overline{\Delta H}^{\theta}_{\mathrm{melt},1}$ are known, x_2^* can be determined from the measured slope of the line. The DSC curve is capable of providing values of F at temperatures T for use in such a plot.

The DSC Melting Curve

The DSC measures the rate of thermal energy transfer, $\mathrm{d}H/\mathrm{d}t$, to or from the sample as the temperature of the sample holder, T, is changed at a constant rate, $\mathrm{d}T/\mathrm{d}t = \phi$. Thus the output from the DSC is directly proportional to the apparent heat capacity of the system, $\mathrm{d}H/\mathrm{d}T$.

$$\frac{\mathrm{d}H}{\mathrm{d}t} = \frac{\mathrm{d}H}{\mathrm{d}T}\cdot\frac{\mathrm{d}T}{\mathrm{d}t} = \phi\cdot\frac{\mathrm{d}H}{\mathrm{d}T} \tag{5}$$

For an absolutely pure compound with zero melting range, $\mathrm{d}H/\mathrm{d}T$ would become infinite at the melting point, T_o. For an impure compound, $\mathrm{d}H/\mathrm{d}T$ is finite and is a function of T.

When the fraction melted, F, is zero, the apparent heat capacity of the sample is that of the solid mixture, and when $F = 1$ the apparent heat capacity of the sample is that of the ideal solution. Intermediate behavior is obtained as follows

$$\frac{\mathrm{d}H}{\mathrm{d}T} = \frac{\mathrm{d}H}{\mathrm{d}F}\cdot\frac{\mathrm{d}F}{\mathrm{d}T}$$

$\mathrm{d}F/\mathrm{d}T$ is obtained from eqn. (3) as

$$\frac{\mathrm{d}F}{\mathrm{d}T} = \frac{x_2^* R T_o^2}{\overline{\Delta H}^{\theta}_{\mathrm{melt},1}(T_o - T)}$$

It is assumed also, because of the restriction to consideration of ideal eutectic systems and to the formation of ideal solutions on melting, that

$$H(F) = \overline{\Delta H}^{\theta}_{\mathrm{melt},1}\cdot F$$

therefore

$$\mathrm{d}H/\mathrm{d}F = \overline{\Delta H}^{\theta}_{\mathrm{melt},1}$$

Combining these results

$$\frac{\mathrm{d}H}{\mathrm{d}T} = \frac{x_2^* R T_o^2}{(T_o - T)^2} \tag{6}$$

Equation (6) then gives the variation of the apparent heat capacity of the sample during melting, as a function of T. The upper limit of the melting process is $T = T_f$ (when $F = 1$). Therefore, from eqn. (4),

$$T_f = T_o - \frac{x_2^* R T_o^2}{\overline{\Delta H}^{\theta}_{\mathrm{melt},1}}$$

The lower limit of the melting process is $T \ll T_o$, when

$$\mathrm{d}H/\mathrm{d}T \simeq x_2^* R = C_s$$

The apparent heat capacity of the sample is approximately constant. In the idealized DSC curves given in Figures 1 and 2, it has been assumed that the heat capacity of the liquid just above the melting temperature is the same as that of the solid at lower temperatures (both equal to C_s).

Since $\mathrm{d}H/\mathrm{d}t$ is proportional to $\mathrm{d}H/\mathrm{d}T$, plots of $\mathrm{d}H/\mathrm{d}T$ against T represent the initial part of an idealized DSC melting curve. Such curves for phenacetin and for benzamide, with values of x_2^* from 0.0050 to 0.3000, have been given by Marti, et al. (*4, 6*).

The real DSC melting curve, because of factors such as thermal lag, which is discussed in more detail below, will look more like the curve in Figure 2, inset. The total area under the curve, the area ABC, is proportional to the enthalpy of fusion, $\overline{\Delta H}^{\theta}_{\mathrm{melt},1}$. The actual value of $\overline{\Delta H}^{\theta}_{\mathrm{melt},1}$ can be obtained by calibration (*8*) of the instrument with a standard of known $\overline{\Delta H}^{\theta}_{\mathrm{melt},1}$ (Fig. 1). The feature sought for the present discussion, the fraction of the sample melted, F, at temperature T, is obtained directly from the fractional area under the curve,

$$F = (\text{area } ADE)/(\text{area } ABC).$$

The range of F values used in practice is usually restricted to $0.1 < F < 0.4$. Even with this restricted range, the linearity of plots of T against $1/F$ (eqn. (4)) is often poor. Corrections have to be made for thermal lag and for undetected premelting, as discussed below.

Thermal Lag

Flow of thermal energy from the holder at the programmed temperature, T_P, to the sample at a slightly lower temperature, T_S, is governed by Newton's law of cooling

$$T_P - T_S = \frac{\mathrm{d}H}{\mathrm{d}t} R_o \tag{7}$$

where R_o is the thermal resistance. The value of R_o for the instrument may be obtained (*9*) from the melting curve of a high purity standard (Fig. 1). This will melt over a very narrow temperature range so that, as the programmed temperature continues to increase with time, the sample temperature, T_S, will remain constant, thus $\mathrm{d}T_S/\mathrm{d}t = 0$. From eqn. (7)

$$\frac{\mathrm{d}T_P}{\mathrm{d}t} - \frac{\mathrm{d}T_S}{\mathrm{d}t} = R_o\frac{\mathrm{d}}{\mathrm{d}t}\left(\frac{\mathrm{d}H}{\mathrm{d}t}\right)$$

Hence,

$$\frac{\mathrm{d}T_P}{\mathrm{d}t} = R_o\frac{\mathrm{d}}{\mathrm{d}t}\left(\frac{\mathrm{d}H}{\mathrm{d}t}\right) = R_o\frac{\mathrm{d}T}{\mathrm{d}t}\cdot\frac{\mathrm{d}}{\mathrm{d}T}\left(\frac{\mathrm{d}H}{\mathrm{d}t}\right) = R_o\phi\frac{\mathrm{d}}{\mathrm{d}T}\left(\frac{\mathrm{d}H}{\mathrm{d}t}\right)$$

and

$$\frac{\mathrm{d}}{\mathrm{d}T}\left(\frac{\mathrm{d}H}{\mathrm{d}t}\right) = \frac{1}{R_o}$$

thus R_o may be determined from the slope, AB, of the DSC melting curve for the high purity standard (Fig. 1). The value of R_o is then used graphically or analytically to correct the programmed temperature, T_P, to the true sample temperature, T_S. T_S then, rather than T_P, is plotted against $1/F$.

Undetermined Premelting

Even with correction for thermal lag, the linearity of the plots of T_S against $1/F$ is often not good. Melting actually begins at the eutectic temperature (line *VW* on Fig. 3, inset), which may be far below the range of temperatures being examined. Corrections thus have to be made to the measured areas, for melting which has occurred at lower temperatures and which is difficult or impossible to measure. This is evident in the small but cumulatively significant deviation from the ideal baseline illustrated in Figure 2.

If the undetermined area under the curve is ϵ, the measured partial areas up to temperature $T_1, T_2, \ldots T_n$ are $a_1, a_2 \ldots a_n$, respectively, and the measured total area is A, the true value of F_n is:

$$F_n = (a_n + \epsilon)/(A + \epsilon)$$

or

$$1/F_n = (A + \epsilon)/(a_n + \epsilon) \simeq A/(a_n + \epsilon),$$

since $A \gg \epsilon$ so the effect of including ϵ is to reduce the value of $1/F_n$, see Figure 4.

In practice ϵ is treated as a parameter whose value is adjusted so that a plot of T_S against the corrected $1/F$ is linear. The restraints are that the final value of $(A + \epsilon)$ should correspond to the correct value of $\overline{\Delta H}^{\theta}_{\mathrm{melt},1}$ (if known) and that the value of T_o, determined from the intercept on the T_S axis, should be correct. Once these conditions have been met, the value of $x_2{}^*$ (= slope × $\overline{\Delta H}^{\theta}_{\mathrm{melt},1}/RT_o^2$) and hence the purity of the sample can be determined. The correction, ϵ, may sometimes be quite large and values of as much as 30% of the total area are not uncommon (*10*). Obviously the approximation, $A + \epsilon \simeq A$, then cannot be used.

The whole procedure for purity determination is summarized in the flowchart (Fig. 5). Computer programs for these calculations have been described (*4, 7, 11*). Cooksey and Hill (*12*) have suggested an alternative procedure for data analysis in which ϵ and $\overline{\Delta H}^{\theta}_{\mathrm{melt},1}$ are eliminated from the calculation and the areas, a_n, are replaced by the ordinates, P_n. Modifications have been suggested also for impurity levels greater than 2% (*13*); for systems where $\overline{\Delta H}^{\theta}_{\mathrm{melt},1}$ varies with temperature or composition (*4, 10*), and for systems where the impurity forms a solid solution (*4, 14*).

Similar determinations have been carried out using adiabatic calorimetry (*15*).

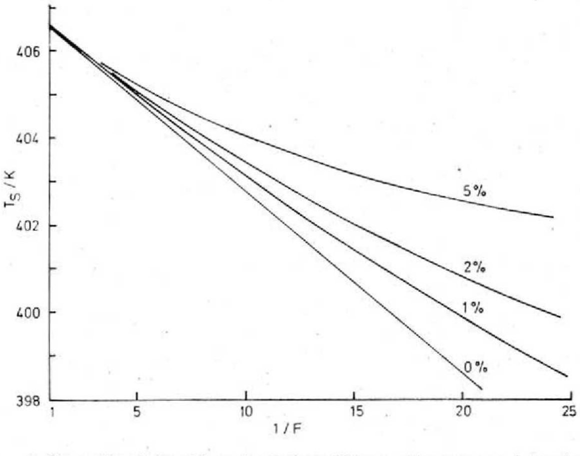

Figure 4. Correction for undetermined premelting: an allowance, ϵ, is made for the area under the curve which has not been accounted for. The fraction of sample melted, F, is equal to $(a + \epsilon)/(A + \epsilon)$, where a is the area measured upto temperature T_S, and A is the total area under the curve. The effect of various values of 100 ϵ/A are shown.

Preparation of the DSC Curves

The DSC curves in Figures 1 and 2 represent idealized scans on *equimolar* quantities (say 0.01 mmol) of very pure indium and of phenacetin, respectively, under identical conditions of chart speed, recorder sensitivity and heating rate. A constant heating rate $\phi = \mathrm{d}T/\mathrm{d}t = 1\ \mathrm{K\ min^{-1}}$ was chosen so that $\mathrm{d}H/\mathrm{d}t = \mathrm{d}H/\mathrm{d}T$. Both curves were constructed in two parts: the region up to the maximum, and the return to the baseline. The return to the baseline is represented by an exponential decay (*14*). For very pure indium (relative atomic mass = 114.8; $T_o = 429.8$ K; $\overline{\Delta H}^{\theta}_{\mathrm{melt,In}} = 3.36\ \mathrm{kJ\ mol^{-1}}$ (8)) the rise to the maximum is taken as linear, that is, $\mathrm{d}H/\mathrm{d}t = \phi t/R_o$ from $t = 0$ at $T = T_o$ to $t = t_{\max}$ at the peak (*14*), see Figure 1. If the maximum value of $\mathrm{d}H/\mathrm{d}t$ is z_R, the return to the baseline is represented by

$$\mathrm{d}H/\mathrm{d}t' = z_R e^{-K_R t'}$$

where $t' = t - t_{\max}$ and $\mathrm{K_R} = 1/(R_o \mathrm{C_R})$, and where C_R is the apparent heat capacity of the reference material (indium) and R_o is the thermal resistance (see above). The values of z_R and $t_{\max}$ are obtained from the condition

$$\textit{Area under peak} = \overline{\Delta H}^{\theta}_{\mathrm{melt,In}} = (R_o z_R^2/2\phi) + z_R R_o C_R \qquad (8)$$

once values for C_{R} and R_o have been decided upon (see below).

Figure 2, for impure phenacetin (relative molar mass 179.2) was constructed on the basis of data given by Marti (4) ($\mathrm{T_o} = 407.0 \pm 0.3$ K; $\overline{\Delta \mathrm{H}}^{\theta}_{\mathrm{melt},1} = 32.4 \pm 1.3\ \mathrm{kJ\ mol^{-1}}$) and for an impurity content, $\mathrm{x_2}^* = 0.05$. (Note that this is a higher content than would normally be treated in practice). At this impurity level, $T_f = 404.88$ K and this would be the true sample temperature, T_S, at the maximum of the melting endotherm. The maximum ordinate of the endotherm $(\mathrm{d}H/\mathrm{d}t)_{\max} = z_S$. The initial part of the DSC curve was then determined from eqn. (6) as a plot of $\mathrm{d}H/\mathrm{d}t$ against t (or T_S) up to $t_{\max}$ at $T_S = T_f = 404.88$ K. Cumulative areas at each T_S may be determined by integration of eqn. (6). At $T = T_f$, the cumulative area corresponds to 95.3% of $\overline{\Delta \mathrm{H}}^{\theta}_{\mathrm{melt},1}$ and $z_S = 153\ \mathrm{mJ\ min^{-1}}$. The return to the baseline is

$$\mathrm{d}H/\mathrm{d}t' = z_S \mathrm{e}^{-K_S t'}$$

where $t' = t - t_{\max}$ and $\mathrm{K_S} = 1/(R_o C_S)$ and where C_S is the apparent heat capacity of the sample. The area of this "tail" should thus be 4.7% of $\overline{\Delta H}^{\theta}_{\mathrm{melt},1}$, so that

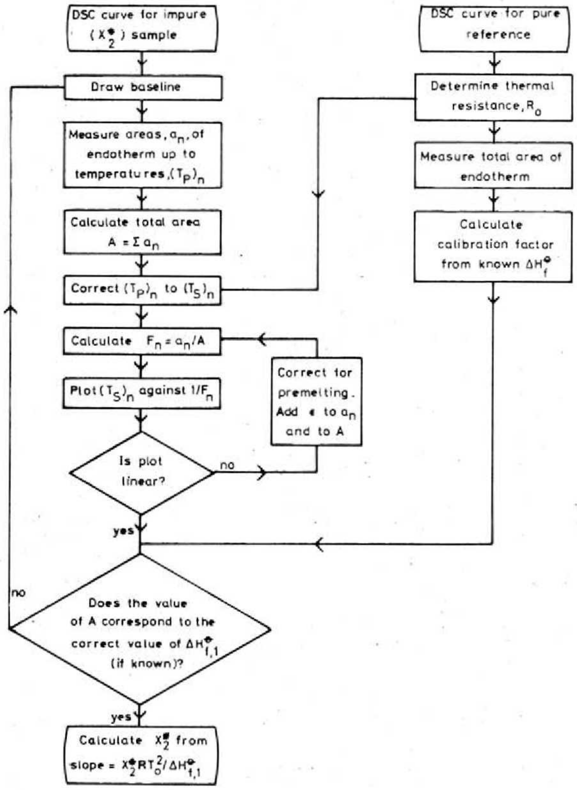

Figure 5. Flowchart representing the procedure used in purity determination by DSC. $\Delta H^{\theta}{}_{f,1} \equiv \overline{\Delta \mathrm{H}}^{\theta}{}_{\mathrm{melt},1}$.

$$\int_0^\infty z_S e^{-K_S t'} dt' = \frac{z_S}{K_S} = z_S R_o C_S = 0.047\ \overline{\Delta H^\theta_{\text{melt},1}} \qquad (9)$$

As the values of C_S and C_R affect mainly the vertical displacements of the DSC curves, it was considered adequate for the present purposes to take $C_S = C_R = 1$ mJ K^{-1}, so that $K_S = K_R/R_o$. From eqn. (9) then, $R_o = 0.0993$ K min mJ^{-1}, and from eqn. (8), $z_R = 72.9$ mJ min^{-1} (and hence t_{max} in Figure 1 is 0.724 min).

The final step in the construction of Figure 2 is to introduce thermal lag (see earlier) into the temperature scale. Line *YB* (Fig. 2) is constructed with the same slope ($= 1/R_o$) as line *AB* in Figure 1. Point *Y* represents the freezing point (sample completely melted) T_f, and should read 404.88 K. Because of thermal lag this value and the whole true sample temperature scale, T_S, will be increased to the programmed temperature, T_P, by a temperature interval *YW*,

$$T_P = T_S + YW$$

A complete table of data for this system is available from the author.

Other DSC curves may be synthesized by varying the impurity content, x_2^*, or for other systems, using the appropriate values of $\overline{\Delta H^\theta_{\text{melt},1}}$ and T_o. Alternatively, actual DSC curves, preferably obtained using the systems so fully studied by Marti (*4, 7*) may be supplied to the student.

Acknowledgment

I am most grateful to Professor L. Glasser for his many helpful comments.

Literature Cited

(1) Smit, W. M., "The Characterization of the Chemical Purity of Organic Compounds," edited by L. A. K. Staveley, Butterworths, London, **1971**, p 7.

(2) Ubbelohde, A. R., "Melting and Crystal Structure," Clarendon Press, Oxford, **1965.**

(3) Johnston, H. L. and Giauque, W. F., *J. Amer. Chem. Soc.*, **51**, 3194 (1929).

(4) Marti, E E., *Thermochim. Acta*, **5**, 173 (1973).

(5) Daniels, T., "Thermal Analysis," Kogan Page, London, **1973.**

(6) Adamson, A. W., "Textbook of Physical Chemistry," Academic Press, New York, **1973,** p 401.

(7) Marti, E. E., Heiber, O., Huber, W. and Tonn, G., "Thermal Analysis," Ed. H. G. Weidemann, Birkhäuser Verlag, Basel, **1971,** Vol. 3, p 83.

(8) Richardson, M. J. and Savill, N. G., *Thermochim. Acta*, **12,** 221 (1975).

(9) *Thermal Analysis Newsletters*, Nos. 5 and 6, Perkin-Elmer Corporation, Norwalk, Connecticut (undated).

(10) Davis, G. J. and Porter, R. S., *J. Thermal Analysis*, 1, 449 (1969).

(11) Moros, S. A. and Stewart, D., *Thermochim. Acta*, **14,** 13 (1976).

(12) Cooksey, B. G., and Hill, R. A. W., *J. Thermal Analysis*, **10,** 83 (1976).

(13) Palermo, E. F. and Chiu, J., *Thermochim. Acta*, **14,** 1 (1976).

(14) Driscoll, G. L., Duling, I. N. and Magnotta, F., "Analytical Calorimetry" (Vol. 1), (Editors: Porter, R. S., and Johnson, J. F.) Plenum, New York, **1968,** p 271.

(15) Westrum, E. F., Jr., in ref. (14), p 231.

(16) Gray, A. P., in ref. (*14*), p 209.